CHINESE OPTICS LETTERS

Vol. 19, No. 11 | November 2021

Liquid crystal devices for vector vortex beams manipulation and quantum information applications [Invited]

Zhi-Xiang Li (李志向)[1], Ya-Ping Ruan (阮亚平)[1], Peng Chen (陈 鹏)[1], Jie Tang (唐 杰)[2], Wei Hu (胡 伟)[1], Ke-Yu Xia (夏可宇)[1], and Yan-Qing Lu (陆延青)[1*]

[1] National Laboratory of Solid State Microstructures, College of Engineering and Applied Sciences, and Collaborative Innovation Center of Advanced Microstructures, Nanjing University, Nanjing 210093, China

[2] School of Science, Nantong University, Nantong 226019, China

*Corresponding author: yqlu@nju.edu.cn

Received August 8, 2021 | Accepted September 6, 2021 | Posted Online October 14, 2021

Vector vortex beams (VVBs) have attracted significant attention in both classical and quantum optics. Liquid crystal (LC), beyond its applications in information display, has emerged as a versatile tool for manipulating VVBs. In this review, we focus on the functions and applications of typical LC devices in recent studies on controlling the space-variant polarized vortex light. Manipulation of VVBs through patterned nematic LC optical elements, patterned cholesteric LC optical elements, self-assembled defects, and LC spatial light modulators is discussed separately. Moreover, LC-based novel optical applications in the field of quantum information are reviewed.

Keywords: liquid crystal; vector beam; *q*-plate; orbital angular momentum; entanglement; two-photon interference.
DOI: 10.3788/COL202119.112601

1. Introduction

Liquid crystal (LC) is an excellent electro-optic material with an intermediate structure between liquids and crystalline solids. It possesses large optical anisotropy, and its optical properties can be easily modified by moderate external fields, allowing amplitude and phase modulations of light. LC display based on modulations of the amplitude or polarization of light has turned out to be a big commercial success. Meanwhile, many novel non-display applications of LC devices have been explored in the field of photonics[1–6]. LC optical elements have found a new role in manipulating different degrees of light, especially in the engineering of vector beams, with the advantages of simple configuration, convenient use, low cost, and high conversion efficiency.

Vector fields[7–9], where the light polarization in the beam transverse plane is space-variant, have attracted much attention. Vector beams arise as natural solutions to the vectorial Helmholtz equation. They are very often generated as the superpositions of orthogonal scalar fields with orthogonal polarization states as

$$\psi(r) = \frac{1}{\sqrt{2}}(|\phi_1\rangle|R\rangle + |\phi_2\rangle|L\rangle), \tag{1}$$

where $|R\rangle$ and $|L\rangle$ represent the right and left circular polarization bases, and $|\phi_1\rangle$ and $|\phi_2\rangle$ are orthogonal scalar fields. One special mode basis that has received great interest is orbital angular momentum (OAM) modes. Light beams carrying OAM are well known as vortex beams. Vortex beams usually have a distribution of homogeneous polarization and possess an azimuthal phase structure in the form of $e^{im\phi}$, where m is the optical topological charge. We have seen tremendous progress and applications with such twisted photons[10–17]. Light beams with an azimuthally varying linear polarization surrounding an optical vortex located on the beam axis, i.e., vector beams with a phase singularity, are called vector vortex beams (VVBs). VVBs are one of the most commonly used vector beams in research nowadays[18–21]. The higher-order Poincaré sphere or hybrid-order Poincaré sphere is usually used to geometrically describe a generalized VVB[22–24]. Compared with the scalar vortex beam and pure vector beam, the VVBs provide more degrees of freedom (DOFs). More importantly, the vector vortex modes are the eigenmodes in an optical fiber, which have robustness of propagation[25,26] and are available for improving the capacity of optical communication systems[27]. In addition, they have applications in beam focusing, particle acceleration, vector vortex filtering, material processing, and quantum information processing[28–31]. Thus, the generation and engineering of vector beams are of particular importance.

This review focuses on different LC elements and their roles in the efficient generation and active control of VVBs. First, we introduce several typical LC optical elements that have been widely used and briefly review recent experimental progress on controlling vector beams. Then, we talk about novel

photonic applications in the quantum domain enabled by LC devices.

2. Manipulation of VVBs by LC Devices

2.1. Patterned nematic LC optical elements

Q-plates are the most commonly used optical elements to generate vector beams[3]. They are also known as vortex retarders. *Q*-plates are essentially a birefringent wave plate with an inhomogeneous distribution of the local optical axis in the transverse plane, and the pattern of the optical axis distribution is defined by a topological charge "q", which can be an integer or half-integer. It is usually operated as half-wavelength spatially variable retarders to achieve the maximum efficiency conversion for a target wavelength. When a circularly polarized light beam passes through a q-plate, $2q\hbar$ amount of OAM is transferred into the beam, with the sign determined by the input polarization helicity[32–36]. Figure 1 shows three examples of q-plate geometries and the illustration of the optical action of a q-plate on a circularly polarized light beam.

Nematic LCs behave optically as uniaxial birefringent media. The director orientation can be controlled externally through electrical biases, optical fields, or surface interactions. Commercially available q-plates utilize nematic LC polymers and require accurate control of thickness during the manufacturing, and generally they are suitable for a single wavelength. Such q-plates feature high integration and are easy to use in the laboratory. Spectral performance of a zero-order LC polymer commercial q-plate has been studied[37]. A recent study has shown that by using different combinations of several commercially available q-plates, different q values can be achieved[38]. Electrically tunable LC q-plates fabricated using photoaligned LC cells provide more flexibility with a wide operating spectrum range, and an arbitrary topological charge can be obtained[39–42]. Radial micro-patterned LC structures fabricated on the basis of the out-of-plane alignment technique also provide electrically tunable generation of VVBs[43].

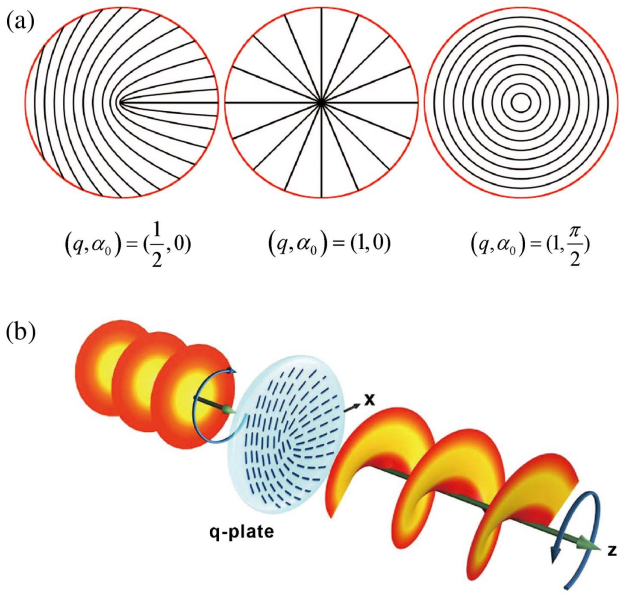

Fig. 1. (a) Three examples of q-plate patterns with α_0 being the initial optical axis orientation, reprinted with permission from Ref. [32], Copyright (2021) by the American Physical Society. (b) Illustration of the optical action of a q-plate with q = 0.5 on left circularly polarized light beam[33].

VVBs can be obtained by simply using a non-circular polarization input beam passing through a q-plate, and the physics behind that is relatively straightforward. Consider a linearly polarized beam carries zero OAM written as $|V\rangle_\pi|0\rangle_o$, where π and o represent polarization and OAM DOF, respectively. The input state can also be written as $\frac{1}{\sqrt{2}}(|R\rangle+|L\rangle)_\pi|0\rangle_o$. After passing through a q-plate, one obtains[34]

$$\frac{1}{\sqrt{2}}(|R\rangle+|L\rangle)_\pi|0\rangle_o \xrightarrow{q-\text{plate}} \frac{1}{\sqrt{2}}(|R\rangle_\pi|-2q\rangle_o+|L\rangle_\pi|2q\rangle_o). \quad (2)$$

This represents a nonseparable state of the polarization and OAM DOFs, which indicates the generation of VVBs.

Figure 2 shows a typical experimental setup to generate and analyze VVBs[44]. Several q-plates with charge $q=0.5$ are used for the generation of VVBs. The waveplates and beam splitter are used to project the beam polarization onto different polarization bases in the analysis process, and a CCD records the corresponding intensity profiles.

Various schemes have been implemented to realize arbitrary VBBs using the LC q-plate. Based on the polarization-guiding effect of the twisted nematic LCs, Chen proposed an LC polarization converter for arbitrary vector beam generation with the combination of one uniformly aligned substrate and a space-variant aligned substrate[44]. The obtained LC converters are further utilized as polarization masks to implement vector-photo-aligning, facilitating the preparation of a q-plate. A VVB can also decompose into a vector beam and a vortex. Liu *et al.*

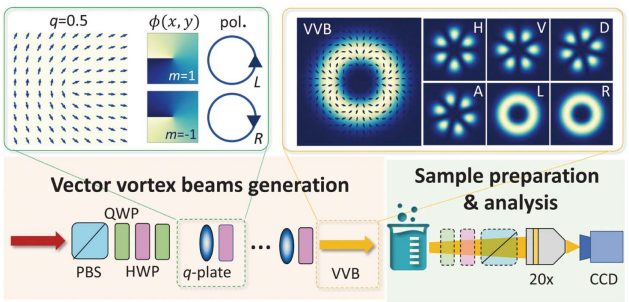

Fig. 2. Experimental scheme to generate and analyze VBBs[45]. The left inset shows the optical axis orientation of one q-plate and the phase acquired by the wavefront in the transverse plane. The right inset shows the intensity distribution of the generated VVB under different polarization. The sample preparation and analysis process are for studying the transmission of VVBs in dispersive media in the original work. PBS, polarized beam splitter; QWP, quarter-wave plate; HWP, half-wave plate; H, horizontal polarization; V, vertical polarization; D, diagonal polarization; A, antidiagonal polarization; L, left circular polarization; and R, right circular polarization.

have proved that combining a q-plate and a spiral phase plate can generate arbitrary VVBs on a hybrid-order Poincaré sphere[46]. Controlled generation of higher-order Poincaré sphere beams from a laser has also been achieved[47]. The Dammann q-plate[48–50], by encoding binary phase into a space-variant geometric phase through a dynamic photopatterning technique in LCs, provides a way for flexible creation of parallel VVBs. Moreover, by combining the uniformly aligned ferroelectric LC with the space-variant photo-patterned nematic LC, the fast switching of OAM and VVBs can be realized[51].

2.2. Patterned cholesteric liquid crystal optical elements

Cholesteric LC (CLC) is a liquid crystalline phase where the rod-like molecules self-assemble into a periodic helical structure and form a natural one-dimensional (1D) soft photonic crystal. The chiral superstructures exhibit a broadband Bragg reflection with unique circular-polarization (spin) selectivity, so it is polychromatic and does not require tuning to maximize the conversion efficiency. Thus, it supplies a new platform for broadband reflective geometric phase manipulation[52–57]. By encoding a specifically designed binary pattern, Chen *et al.* demonstrated an innovative CLC optical vortex processor[58,59]. They extracted up to 25 different vortices with equal efficiency over a wavelength range of 116 nm. Recently, based on a chirality invertible self-organized CLC superstructure, they demonstrated on-demand beam tailoring and showed various light-driven geometric phase elements such as deflector, lens, Airy beam, and OAM generators[60]. These works advance the fundamental understanding of ordered soft matter and allow us to explore more fantastic applications.

For a long time, the vector beam generation has not been announced by the CLC q-plate because flipping the incident circular polarization state does not imply the Berry phase reversal[61]. This fundamental limitation prevents the generation of vector beams from homogeneous linear polarization based on a CLC device with monotonous chirality. With the assistance of a rear mirror, Rafayelyan created a Bragg Berry q-plate[62], which allows broadband spin-to-OAM mapping.

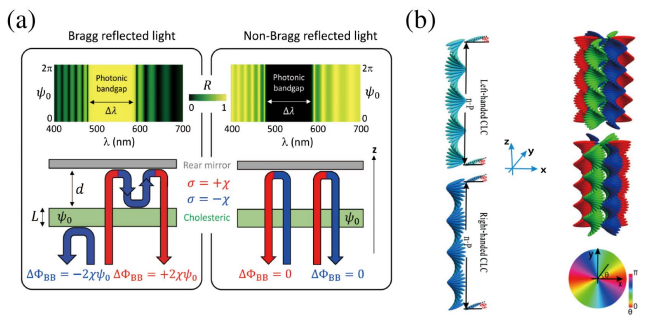

Fig. 3. Different schemes to generate vector beams using CLC. (a) Generic mirror-backed Bragg–Berry optical element, reprinted with permission from Ref. [62]. Copyright (2021) by the American Physical Society. (b) Stacking two opposite-handed CLCs, reprinted with permission from Ref. [63]. Copyright (2019) by The Optical Society.

In their work, incident light with helicity $\sigma = +\chi$ is transmitted through the cholesteric and then reflected by the rear mirror with a flipped helicity. While for the incident helicity $\sigma = -\chi$, light propagating along the helix axis experiences helicity-preserved Bragg reflection. As shown in Fig. 3(a), arbitrarily polarized light is fully Bragg reflected for optical frequencies inside the band gap, while only a fraction of the incident light is Bragg reflected outside the band gap. Another work to overcome the limitation of CLC reflectivity is by stacking two opposite-handed CLCs with the same pitches and the same surface azimuthal angles[63], as shown in Fig. 3(b). They demonstrated the VVBs generation via input light with homogeneous linear polarization interacting through the proposed structure. These works verify that CLCs can also be used to generate vector beams in a robust and direct way.

2.3. Self-assembled defects

LCs are capable of self-assembly due to their orientation elasticity, and spontaneously formed LC topological defects under external fields offer a nature-assisted route to the creation of geometric phase optical elements. Through exploitation of topological defects, optical vortex generation can be achieved by the transfer of the topological singularity from the director structure to the light phase[64–71].

Migara *et al.* demonstrated a simple method to create a stable and rewritable defect in a vertically aligned LC cell using external point pressure, and such an LC defect also serves as q-plates[67]. Using initially homogeneous nematic LC films under the influence of a magneto-electric external field, Brasselet demonstrated self-engineered q-plates (shown in Fig. 4) with electrically tunable operating wavelength[72]. The process is technology-free and results in high resolution.

Self-assembled topological defects could also operate as a nonlinear protocol to manipulate high-dimensional spin-orbit optical states. In practice, a q-plate is a linear optical element. By exploiting both the giant optical orientational nonlinearities

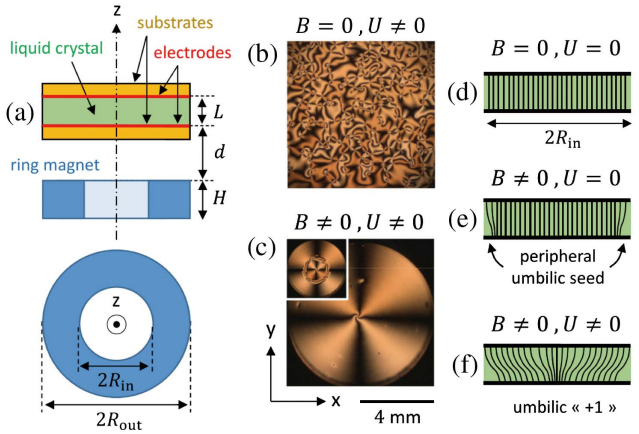

Fig. 4. Experimental scheme to generate self-engineered LC q-plates. Reprinted with permission from Ref. [72]. Copyright (2021) by the American Physical Society.

of LCs and their ability to self-organize into topological defects, control of vector beams in a nonlinear manner was proposed and experimentally demonstrated[73]. A tunable optical vortex generator based on a grid-patterned LC cell has been demonstrated recently, with the ability to generate and manipulate an array of optical vortex beams[74].

Compared to patterned nematic or CLC q-plates, extra orientation techniques are not needed in such soft-matter self-organization processes. Besides, they are robust and cost-effective. With the progress made in large-scale self-organization of reconfigurable topological defect networks in LCs[75] and tunable two-dimensional (2D) self-organized patterns[76], the corresponding applications in optical vector beam shaping are promising.

2.4. Liquid-crystal spatial light modulators

Spatial light modulators (SLMs) are pixelated devices, and each pixel can be programmed to introduce certain phase delay to the output light. SLMs allow for real-time manipulation of both the phase and amplitude of light field by computer-generated holograms. It has become a powerful tool for on-demand generation and analysis of arbitrary optical modes[77].

The basic principle to generate VVBs is by using a phase-only SLM based on the superposition of two components with the orthogonal circular polarization basis[78–82]. A beam incident on an SLM is divided into two orthogonal polarization components, each of which is imparted to the designed phase, and then they are recombined to yield the desired vector beam. Despite the flexibility in various photonic applications, the conversion efficiency of SLMs is generally low because of the diffraction process. However, one can select a blazing grating to improve diffraction efficiency[8] or employ two SLMs in a common-path architecture[79]. An optical arrangement containing a triangular common-path interferometer [Fig. 5(a)] has been proposed to overcome this problem, and the conversion efficiency is about 47% in the experiment[80]. Figure 5(b) shows another method to efficiently generate VVBs with a single ultra-high-definition phase-only SLM and a single polarized beam splitter (PBS)[81].

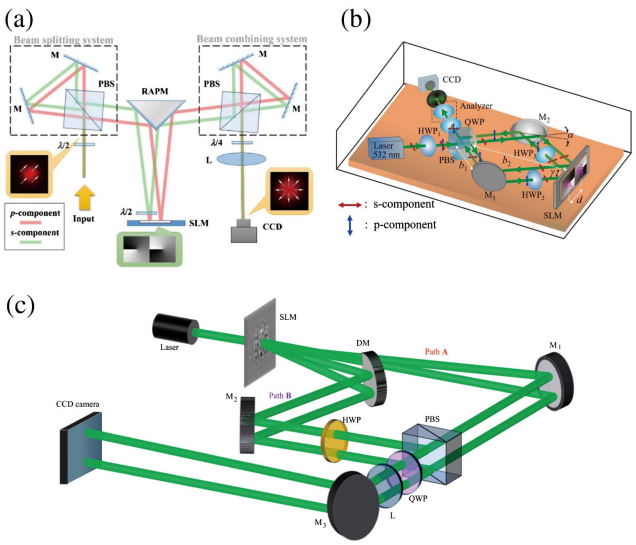

Fig. 5. Experimental setups for generating vector beams using SLMs. (a) Experimental setup for generating arbitrary vector beams via a triangular common-path interferometer[80]; (b) generation of arbitrary vector beams by interferometric methods using a single SLM, reprinted with permission from Ref. [81]. Copyright (2019) by The Optical Society. (c) Schematic representation to generate multiple vector beams by the use of an SLM, reprinted with permission from Ref. [82]. Copyright (2019) by The Optical Society.

Besides the efforts to optimize the generation efficiency of the structured light through SLM, simultaneous generation of many vector beams using a single digital hologram was pursued[82] [Fig. 5(c)]. The generation of perfect vectorial vortex beams has been realized[83].

Although both LC-based q-plates and SLMs can generate VVBs, they are different in principle, as the SLM is based on dynamic phase manipulation, while q-plates are geometric phase elements. However, by utilizing the sensitivity of SLMs to polarization with a double pass experimental setup, a q-plate equivalent system can be realized by a transmissive SLM, capable of generating programmable vector beams with arbitrary q[84].

3. Applications of LC devices in quantum regime

LC optical elements have played important roles in the field of quantum optics. Here, we mainly discuss their roles in the generation of various entanglement structures and their applications in the field of two-photon interference.

3.1. Generation of various entanglement structures

LC q-plates can be used in the generation of nonseparable states in the quantum regime[85,86]. A key characteristic of vector fields is the coupling between the polarization and the spatial mode: in contrast to scalar fields, these DOFs are nonseparable. The concept of classical entanglement or intra-system entanglement is used to describe such properties of vector beams, as it is mathematically equivalent to quantum entanglement. However, non-locality is not involved in different DOFs of one entity. A complete discussion about classical entanglement lies beyond the scope of this review; one can find details from Refs. [87–92]. In the study of the state evolution of classically entangled DOFs in atmospheric turbulence[93], entangled qubits were encoded and decoded using q-plates. At the same time, the nonseparability of vector vortex modes was measured by using an SLM.

Utilizing patterned LC q-plates, Parigi *et al.* realized the storage and retrieval of vector beams at the single-photon level in laser-cooled atoms[94]. They used q-plates in both generation and detection processes. The generated vector state was converted to a polarization state and analyzed by exploiting a second q-plate and standard polarization optics. Li *et al.* demonstrated the heralded storage of single-photon hybrid entanglement in a solid-state medium with the help of SLM[95].

Combining entangled photon pairs generated through a spontaneous parametric down-conversion (PDC) process with VVBs generated via q-plates, D'Ambrosio and coworkers have thoroughly studied the properties of two entangled VVBs[96]. Their investigation indicates that the complex polarization pattern is a manifestation of intra-system entanglement between polarization and OAM. In contrast, the inter-system entanglement between two vectorial fields can be used in different quantum scenarios and is worth more exploration. An intra-city link in Ottawa was built to test the high-dimensional quantum key distribution outside of a laboratory, and q-plates were utilized in the process to prepare the initial quantum states[97].

Graffitti *et al.* demonstrated a novel scheme for efficient generation of a complex entanglement structure between three DOFs of light. Combining time-frequency mode (TFM) encoding through a PDC process and VVB encoding via a q-plate, they generated a simple yet high-quality source of TFM-VVB hyperentanglement[98]. The sketch of the biphoton hyperentangled state is shown in Fig. 6.

The multiplexing of vector beams by SLMs has attracted much attention lately[99–101], providing the potential to further increase the data transmission rate. Otte and coworkers demonstrated a practical example of engineered generation and propagation of a light field enabled by such a multiplexing technique[102]. By combining two orthogonal vector beams, a light field with a z-dependent degree of entanglement is generated (Fig. 7), and such a field manifests itself through a change in the degree of local entanglement during propagation in free space. In their experiment, digital propagation of a light field is also achieved by the use of an SLM and a lens based on the Fourier transform.

LC devices also play an invaluable role in the research of quantum walks for simulations of quantum dynamics[103–105], which has been used to generate high-dimensional quantum states lately[106–109]. Experimental engineering of arbitrary qudit states based on quantum walks was demonstrated[107], with five q-plates implementing the shift operator of the quantum walk. Giordani proposed an entanglement transfer protocol from low- to high-dimensional DOFs via quantum-walk-based

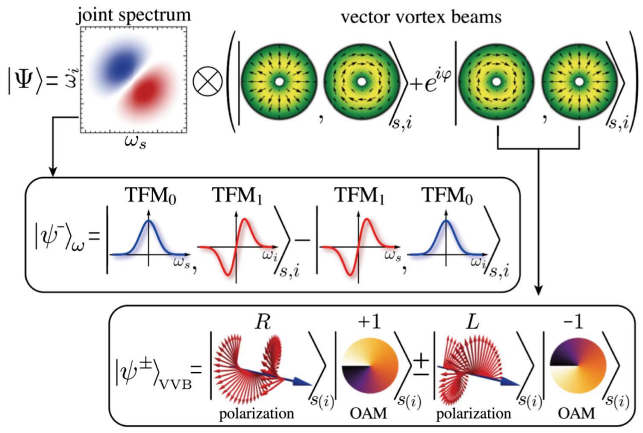

Fig. 6. Sketch of the biphoton hyperentangled state[98].

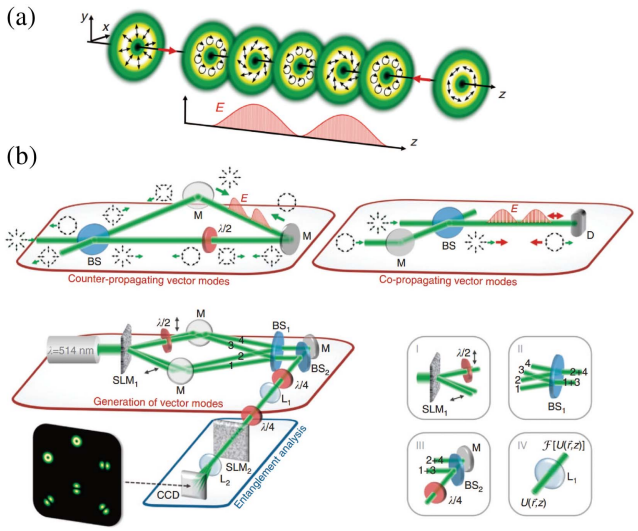

Fig. 7. Schematic representation of the investigated field with a z-dependent degree of entanglement[102]. (a) Basic concept with a z-dependent degree of entanglement. (b) Experimental scheme.

qubit–qudit dynamics[108]. The flexibility of LC devices has been perfectly demonstrated in the field of high-dimensional entanglement generations.

3.2. Applications in two-photon interference

The Hong–Ou–Mandel (HOM) effect is a two-photon interference effect and is widely regarded as the quintessential quantum interference phenomenon in optics. It manifests as the bunching/antibunching of two indistinguishable photons upon mixing at a mode splitter. It is fundamentally interesting, as it has no classical counterpart, and it is at the heart of many applications ranging from precision measurement to quantum computations and communication[110].

LC optical elements offer a convenient way to control the HOM effect. HOM interference of scalar OAM states has also been demonstrated by the use of a q-plate[111]. In 2019, by tuning two parameters of a q-plate, a tunable HOM interference between vectorial modes of light has been achieved[112]. The transformation induced by a q-plate on VVBs can be represented by an orbit on the corresponding hybrid Poincaré sphere (Fig. 8). Two-photon interferences in high-dimensional mode have also been studied. Three SLMs are used for spatial mode generation, unitary transformation, and measurement separately[113] (Fig. 9). These works prove the versatile application of LC devices for quantum information tasks.

4. Summary and Outlook

In this short review, we have discussed and compared various LC optical devices for the generation and manipulation of VVBs. The quantum applications of LCs are reviewed, and the functions of various LC devices are discussed in different scenarios.

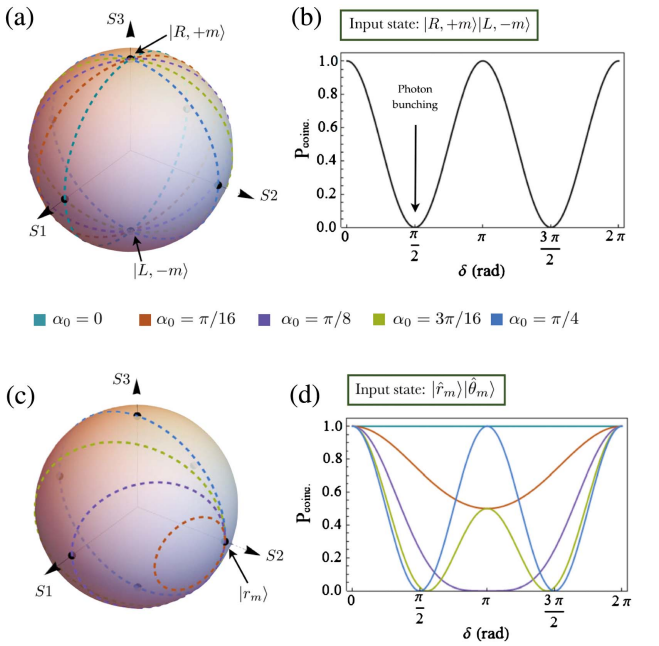

Fig. 8. Tunable two-photon quantum interference by using a *q*-plate[112]. Different transformation orbits for different angles α_0 when the input photon states lie (a) on the poles and (c) on the equator; (b) and (d) represent the two photon coincidence probabilities for the corresponding orbits by changing the *q*-plate phase. Reprinted with permission from Ref. [112]. Copyright (2021) by the American Physical Society.

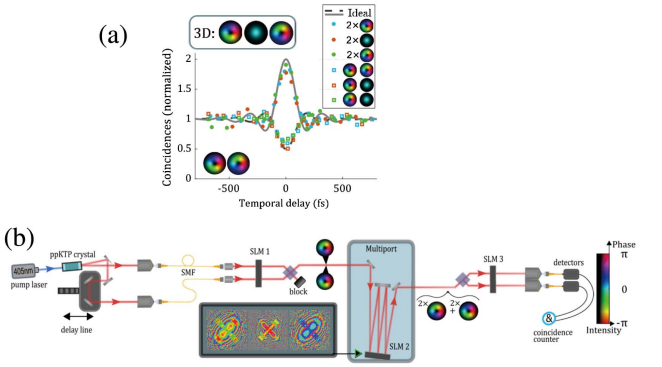

Fig. 9. Application of SLMs in high-dimensional two-photon interference[113]. (a) Two-photon interference in a 3D mode splitter. (b) Experimental setup. Reprinted with permission from Ref. [114]. Copyright (2021) by the American Physical Society.

In the future, with the advantage of their flexible tuning property, LCs will continually serve as important tools for quantum information tasks, notably in a controlled and programmable fashion. Apart from its promising applications in engineering complex entanglement structures and high-dimensional quantum states, wavelength-tunable single-photon sources could also be pursued[114,115].

Besides the applications of LC devices in the field of VVBs engineering, manipulations of other types of vector beams are worth exploring. For example, an LC *q*-symmetric-Airy plate is fabricated to generate symmetric Airy vector beams[116]. Möbius strips of optical polarization have been successfully generated by tightly focusing the light beam emerging from a *q*-plate[117], which expands applications of optical LC *q*-plates from 2D field polarization structures to 3D cases. Moreover, recent advances in active and multifunctional LC planar optics[6] may offer new possibilities for photon shaping.

LC layers integrated into metasurfaces have attracted much attention and brought additional active functionalities[118,119]. The graded-index waveguide has also been successfully fabricated using LCs[120]. Novel structures taking advantages of both LC and other materials may lead to promising applications in integration optics. The collaboration of nonlinear processes in lithium niobate and space-variant LC, allowing dynamic switching between the Airy beam and Airy vortex beam in the second-harmonic generation process[121], provides a novel way to achieve dynamic steering of nonlinear structured light.

Despite all the progress made so far, the potential of photon engineering based on LC elements is far from fully exploited. With the continuous innovation of LC technology, exciting new applications will surely follow.

Acknowledgement

This work was supported by the National Key Research and Development Program of China (Nos. 2017YFA0303700 and 2019YFA0308700), the National Natural Science Foundation of China (NSFC) (Nos. 11874212, 11890704, 62035008, 12004175, and 62175101), and the Natural Science Foundation of Jiangsu Province (No. BK20200311).

References

1. C.-C. Lee, *The Current Trends of Optics and Photonics* (Springer Netherlands, 2015).
2. J. M. Otón, E. Otón, X. Quintana, and M. A. Geday, "Liquid-crystal phase-only devices," J. Mol. Liq. **267**, 469 (2018).
3. A. Rubano, F. Cardano, B. Piccirillo, and L. Marrucci, "*Q*-plate technology: a progress review [Invited]," J. Opt. Soc. Am. B **36**, D70 (2019).
4. A. Márquez and Á. Lizana, "Special issue on liquid crystal on silicon devices: modeling and advanced spatial light modulation applications," Appl. Sci. **9**, 3049 (2019).
5. G. Lazarev, P.-J. Chen, J. Strauss, N. Fontaine, and A. Forbes, "Beyond the display: phase-only liquid crystal on silicon devices and their applications in photonics [Invited]," Opt. Express **27**, 16206 (2019).
6. P. Chen, B. Wei, W. Hu, and Y. Lu, "Liquid-crystal-mediated geometric phase: from transmissive to broadband reflective planar optics," Adv. Mater. **32**, 1903665 (2020).
7. J. Chen, C. Wan, and Q. Zhan, "Vectorial optical fields: recent advances and future prospects," Sci. Bull. **63**, 54 (2018).
8. C. Maurer, A. Jesacher, S. Fürhapter, S. Bernet, and M. Ritsch-Marte, "Tailoring of arbitrary optical vector beams," New J. Phys. **9**, 78 (2007).
9. A. Forbes, "Structured light from lasers," Laser Photon. Rev. **13**, 1900140 (2019).
10. X. Wang, Z. Nie, Y. Liang, J. Wang, T. Li, and B. Jia, "Recent advances on optical vortex generation," Nanophotonics **7**, 1533 (2018).
11. Z. Yang, O. S. Magaña-Loaiza, M. Mirhosseini, Y. Zhou, B. Gao, L. Gao, S. M. H. Rafsanjani, G.-L. Long, and R. W. Boyd, "Digital spiral object identification using random light," Light Sci. Appl. **6**, e17013 (2017).

12. X. Qiu, F. Li, W. Zhang, Z. Zhu, and L. Chen, "Spiral phase contrast imaging in nonlinear optics: seeing phase objects using invisible illumination," Optica **5**, 208 (2018).
13. X. Qiu, D. Zhang, W. Zhang, and L. Chen, "Structured-pump-enabled quantum pattern recognition," Phys. Rev. Lett. **122**, 123901 (2019).
14. R. Fickler, G. Campbell, B. Buchler, P. K. Lam, and A. Zeilinger, "Quantum entanglement of angular momentum states with quantum numbers up to 10,010," Proc. Natl. Acad. Sci. USA **113**, 13642 (2016).
15. J. Wang, "Twisted optical communications using orbital angular momentum," Sci. Chin. Phys. Mech. Astron. **62**, 34201 (2019).
16. M. Erhard, R. Fickler, M. Krenn, and A. Zeilinger, "Twisted photons: new quantum perspectives in high dimensions," Light Sci. Appl. **7**, 17146 (2018).
17. X. Fang, H. Ren, and M. Gu, "Orbital angular momentum holography for high-security encryption," Nat. Photon. **10**, 2986 (2019).
18. T. D. Huang and T. H. Lu, "Controlling an optical vortex array from a vortex phase plate, mode converter, and spatial light modulator," Opt. Lett. **44**, 3917 (2019).
19. A. Komar, Z. Fang, J. Bohn, J. Sautter, M. Decker, A. Miroshnichenko, T. Pertsch, I. Brener, Y. S. Kivshar, I. Staude, and D. N. Neshev, "Electrically tunable all-dielectric optical metasurfaces based on liquid crystals," Appl. Phys. Lett. **110**, 071109 (2017).
20. D. Wang, F. Liu, T. Liu, S. Sun, Q. He, and L. Zhou, "Efficient generation of complex vectorial optical fields with metasurfaces," Light Sci. Appl. **10**, 67 (2021).
21. Y. Chen, K.-Y. Xia, W.-G. Shen, J. Gao, Z.-Q. Yan, Z.-Q. Jiao, J.-P. Dou, H. Tang, Y.-Q. Lu, and X.-M. Jin, "Vector vortex beam emitter embedded in a photonic chip," Phys. Rev. Lett. **124**, 153601 (2020).
22. X. Yi, Y. Liu, X. Ling, X. Zhou, Y. Ke, H. Luo, S. Wen, and D. Fan, "Hybrid-order Poincaré sphere," Phys. Rev. A **91**, 023801 (2015).
23. G. Milione, S. Evans, D. A. Nolan, and R. R. Alfano, "Higher order Pancharatnam–Berry phase and the angular momentum of light," Phys. Rev. Lett. **108**, 190401 (2012).
24. G. Milione, H. I. Sztul, D. A. Nolan, and R. R. Alfano, "Higher-order Poincaré sphere, Stokes parameters, and the angular momentum of light," Phys. Rev. Lett. **107**, 053601 (2011).
25. B. Ndagano, R. Brüning, M. McLaren, M. Duparré, and A. Forbes, "Fiber propagation of vector modes," Opt. Express **23**, 17330 (2015).
26. W. Qiao, T. Lei, Z. Wu, S. Gao, Z. Li, and X. Yuan, "Approach to multiplexing fiber communication with cylindrical vector beams," Opt. Lett. **42**, 2579 (2017).
27. G. Milione, M. P. J. Lavery, H. Huang, Y. Ren, G. Xie, T. A. Nguyen, E. Karimi, L. Marrucci, D. A. Nolan, R. R. Alfano, and A. E. Willner, "4 × 20 Gbit/s mode division multiplexing over free space using vector modes and a *q*-plate mode (de)multiplexer," Opt. Lett. **40**, 1980 (2015).
28. M. McLaren, T. Konrad, and A. Forbes, "Measuring the nonseparability of vector vortex beams," Phys. Rev. A **92**, 023833 (2015).
29. B. Ndagano, I. Nape, M. A. Cox, C. Rosales-Guzman, and A. Forbes, "Creation and detection of vector vortex modes for classical and quantum communication," J. Lightwave Technol. **36**, 292 (2018).
30. C. Rosales-Guzmán, B. Ndagano, and A. Forbes, "A review of complex vector light fields and their applications," J. Opt. **20**, 123001 (2018).
31. P. Yue, D. Jianping, and W. Huitian, "Manipulation on novel vector optical fields: introduction, advances and applications," Acta Opt. Sin. **39**, 0126001 (2019).
32. W. Ji, C.-H. Lee, P. Chen, W. Hu, Y. Ming, L. Zhang, T.-H. Lin, V. Chigrinov, and Y.-Q. Lu, "Meta-*q*-plate for complex beam shaping," Sci. Rep. **6**, 25528 (2016).
33. L. Marrucci, C. Manzo, and D. Paparo, "Optical spin-to-orbital angular momentum conversion in inhomogeneous anisotropic media," Phys. Rev. Lett. **96**, 163905 (2006).
34. L. Marrucci, E. Karimi, S. Slussarenko, B. Piccirillo, E. Santamato, E. Nagali, and F. Sciarrino, "Spin-to-orbital conversion of the angular momentum of light and its classical and quantum applications," J. Opt. **13**, 064001 (2011).
35. E. Cohen, H. Larocque, F. Bouchard, F. Nejadsattari, Y. Gefen, and E. Karimi, "Geometric phase from Aharonov–Bohm to Pancharatnam–Berry and beyond," Nat. Rev. Phys. **1**, 437 (2019).
36. L. Marrucci, E. Nagali, F. Sciarrino, L. Sansoni, F. De Martini, B. Piccirillo, E. Karimi, and E. Santamato, "Photonic quantum information applications of patterned liquid crystals," Mol. Cryst. Liq. Cryst. **526**, 108 (2010).
37. M. M. Sánchez-López, I. Abella, D. Puerto-García, J. A. Davis, and I. Moreno, "Spectral performance of a zero-order liquid-crystal polymer commercial *q*-plate for the generation of vector beams at different wavelengths," Opt. Laser Technol. **106**, 168 (2018).
38. S. Delaney, M. M. Sánchez-López, I. Moreno, and J. A. Davis, "Arithmetic with *q*-plates," Appl. Opt. **56**, 596 (2017).
39. S. Slussarenko, A. Murauski, T. Du, V. Chigrinov, L. Marrucci, and E. Santamato, "Tunable liquid crystal *q*-plates with arbitrary topological charge," Opt. Express **19**, 4085 (2011).
40. W. Ji, B.-Y. Wei, P. Chen, W. Hu, and Y.-Q. Lu, "Optical field control via liquid crystal photoalignment," Mol. Cryst. Liq. Cryst. **644**, 3 (2017).
41. S. Ge, P. Chen, Z. Shen, W. Sun, X. Wang, W. Hu, Y. Zhang, and Y. Lu, "Terahertz vortex beam generator based on a photopatterned large birefringence liquid crystal," Opt. Express **25**, 12349 (2017).
42. B.-Y. Wei, S. Liu, P. Chen, S.-X. Qi, Y. Zhang, W. Hu, Y.-Q. Lu, and J.-L. Zhao, "Vortex Airy beams directly generated via liquid crystal *q*-Airy-plates," Appl. Phys. Lett. **112**, 121101 (2018).
43. Z. Ji, X. Zhang, Y. Zhang, Z. Wang, I. Drevensek-Olenik, R. Rupp, W. Li, Q. Wu, and J. Xu, "Electrically tunable generation of vectorial vortex beams with micro-patterned liquid crystal structures," Chin. Opt. Lett. **15**, 070501 (2017).
44. P. Chen, W. Ji, B.-Y. Wei, W. Hu, V. Chigrinov, and Y.-Q. Lu, "Generation of arbitrary vector beams with liquid crystal polarization converters and vector-photoaligned *q*-plates," Appl. Phys. Lett. **107**, 241102 (2015).
45. I. Gianani, A. Suprano, T. Giordani, N. Spagnolo, F. Sciarrino, D. Gorpas, V. Ntziachristos, K. Pinker, N. Biton, J. Kupferman, and S. Arnon, "Transmission of vector vortex beams in dispersive media," Adv. Photon. **2**, 036003 (2020).
46. Z. Liu, Y. Liu, Y. Ke, Y. Liu, W. Shu, H. Luo, and S. Wen, "Generation of arbitrary vector vortex beams on hybrid-order Poincaré sphere," Photon. Res. **5**, 15 (2017).
47. D. Naidoo, F. S. Roux, A. Dudley, I. Litvin, B. Piccirillo, L. Marrucci, and A. Forbes, "Controlled generation of higher-order Poincaré sphere beams from a laser," Nat. Photon. **10**, 327 (2016).
48. P. Chen, S.-J. Ge, W. Duan, B.-Y. Wei, G.-X. Cui, W. Hu, and Y.-Q. Lu, "Digitalized geometric phases for parallel optical spin and orbital angular momentum encoding," ACS Photon. **4**, 1333 (2017).
49. P. Chen, S. Ge, L. Ma, W. Hu, V. Chigrinov, and Y. Lu, "Generation of equal-energy orbital angular momentum beams via photopatterned liquid crystals," Phys. Rev. Appl. **5**, 044009 (2016).
50. Y.-H. Zhang, P. Chen, S.-J. Ge, T. Wei, J. Tang, W. Hu, and Y.-Q. Lu, "Spin-controlled massive channels of hybrid-order Poincaré sphere beams," Appl. Phys. Lett. **117**, 081101 (2020).
51. Y. Liu, P. Chen, R. Yuan, C.-Q. Ma, Q. Guo, W. Duan, V. G. Chigrinov, W. Hu, and Y.-Q. Lu, "Ferroelectric liquid crystal mediated fast switchable orbital angular momentum of light," Opt. Express **27**, 36903 (2019).
52. M. Rafayelyan, G. Agez, and E. Brasselet, "Ultrabroadband gradient-pitch Bragg–Berry mirrors," Phys. Rev. A **96**, 043862 (2017).
53. J. Kobashi, H. Yoshida, and M. Ozaki, "Polychromatic optical vortex generation from patterned cholesteric liquid crystals," Phys. Rev. Lett. **116**, 253903 (2016).
54. J. Kobashi, H. Yoshida, and M. Ozaki, "Planar optics with patterned chiral liquid crystals," Nat. Photon. **10**, 389 (2016).
55. M. Rafayelyan, G. Tkachenko, and E. Brasselet, "Reflective spin-orbit geometric phase from chiral anisotropic optical media," Phys. Rev. Lett. **116**, 253902 (2016).
56. R. Barboza, U. Bortolozzo, M. G. Clerc, and S. Residori, "Berry phase of light under Bragg reflection by chiral liquid-crystal media," Phys. Rev. Lett. **117**, 053903 (2016).
57. C. Yuan, W. Huang, X. Wang, D. Shen, and Z. Zheng, "Electrically tunable helicity of cholesteric heliconical superstructure [Invited]," Chin. Opt. Lett. **18**, 080005 (2020).
58. P. Chen, L.-L. Ma, W. Duan, J. Chen, S.-J. Ge, Z.-H. Zhu, M.-J. Tang, R. Xu, W. Gao, T. Li, W. Hu, and Y.-Q. Lu, "Digitalizing self-assembled chiral superstructures for optical vortex processing," Adv. Mater. **30**, 1705865 (2018).
59. C.-T. Xu, P. Chen, Y.-H. Zhang, X.-Y. Fan, Y.-Q. Lu, and W. Hu, "Tunable band-pass optical vortex processor enabled by wash-out-refill chiral superstructures," Appl. Phys. Lett. **118**, 151102 (2021).

60. P. Chen, L.-L. Ma, W. Hu, Z.-X. Shen, H. K. Bisoyi, S.-B. Wu, S.-J. Ge, Q. Li, and Y.-Q. Lu, "Chirality invertible superstructure mediated active planar optics," Nat. Commun. **10**, 2518 (2019).
61. M. Rafayelyan and E. Brasselet, "Bragg–Berry mirrors: reflective broadband *q*-plates," Opt. Lett. **41**, 3972 (2016).
62. M. Rafayelyan and E. Brasselet, "Spin-to-orbital angular momentum mapping of polychromatic light," Phys. Rev. Lett. **120**, 213903 (2018).
63. T. Lin, Y. Yuan, Y. Zhou, W. Fu, H. Huang, L. Yao, F. Fan, and S. Wen, "Bragg reflective polychromatic vector beam generation from opposite-handed cholesteric liquid crystals," Opt. Lett. **44**, 2720 (2019).
64. R. Barboza, U. Bortolozzo, M. G. Clerc, S. Residori, and E. Vidal-Henriquez, "Optical vortex induction via light–matter interaction in liquid-crystal media," Adv. Opt. Photon. **7**, 635 (2015).
65. E. Brasselet, "Tunable optical vortex arrays from a single nematic topological defect," Phys. Rev. Lett. **108**, 087801 (2012).
66. P. Salamon, N. Éber, Y. Sasaki, H. Orihara, Á. Buka, and F. Araoka, "Tunable optical vortices generated by self-assembled defect structures in nematics," Phys. Rev. Appl. **10**, 044008 (2018).
67. L. K. Migara, H. Lee, C.-M. Lee, K. Kwak, D. Lee, and J.-K. Song, "External pressure induced liquid crystal defects for optical vortex generation," AIP Adv. **8**, 065219 (2018).
68. E. Brasselet, N. Murazawa, H. Misawa, and S. Juodkazis, "Optical vortices from liquid crystal droplets," Phys. Rev. Lett. **103**, 103903 (2009).
69. E. Brasselet and C. Loussert, "Electrically controlled topological defects in liquid crystals as tunable spin-orbit encoders for photons," Opt. Lett. **36**, 719 (2011).
70. B. Son, S. Kim, Y. H. Kim, K. Käläntär, H.-M. Kim, H.-S. Jeong, S. Q. Choi, J. Shin, H.-T. Jung, and Y.-H. Lee, "Optical vortex arrays from smectic liquid crystals," Opt. Express **22**, 4699 (2014).
71. N. Kravets and E. Brasselet, "Taming the swirl of self-structured liquid crystal *q*-plates," J. Opt. **22**, 34001 (2020).
72. E. Brasselet, "Tunable high-resolution macroscopic self-engineered geometric phase optical elements," Phys. Rev. Lett. **121**, 033901 (2018).
73. N. Kravets and E. Brasselet, "Nonlinear unitary transformations of space-variant polarized light fields from self-induced geometric-phase optical elements," Phys. Rev. A **97**, 013834 (2018).
74. D. Lee, H. Lee, L. K. Migara, K. Kwak, V. P. Panov, and J. Song, "Widely tunable optical vortex array generator based on grid patterned liquid crystal cell," Adv. Opt. Mater. **9**, 2001604 (2021).
75. Y. Sasaki, V. S. R. Jampani, C. Tanaka, N. Sakurai, S. Sakane, K. V. Le, F. Araoka, and H. Orihara, "Large-scale self-organization of reconfigurable topological defect networks in nematic liquid crystals," Nat. Commun. **7**, 13238 (2016).
76. R. Amano, P. Salamon, S. Yokokawa, F. Kobayashi, Y. Sasaki, S. Fujii, Á. Buka, F. Araoka, and H. Orihara, "Tunable two-dimensional polarization grating using a self-organized micropixelated liquid crystal structure," RSC Adv. **8**, 41472 (2018).
77. A. Forbes, A. Dudley, and M. McLaren, "Creation and detection of optical modes with spatial light modulators," Adv. Opt. Photon. **8**, 200 (2016).
78. X.-L. Wang, J. Ding, W.-J. Ni, C.-S. Guo, and H.-T. Wang, "Generation of arbitrary vector beams with a spatial light modulator and a common path interferometric arrangement," Opt. Lett. **32**, 3549 (2007).
79. P. García-Martínez, D. Marco, J. L. Martínez-Fuentes, M. del Mar Sánchez-López, and I. Moreno, "Efficient on-axis SLM engineering of optical vector modes," Opt. Lasers Eng. **125**, 105859 (2020).
80. S. Liu, S. Qi, Y. Zhang, P. Li, D. Wu, L. Han, and J. Zhao, "Highly efficient generation of arbitrary vector beams with tunable polarization, phase, and amplitude," Photon. Res. **6**, 228 (2018).
81. Y. Gao, Z. Chen, J. Ding, and H.-T. Wang, "Single ultra-high-definition spatial light modulator enabling highly efficient generation of fully structured vector beams," Appl. Opt. **58**, 6591 (2019).
82. C. Rosales-Guzmán, N. Bhebhe, and A. Forbes, "Simultaneous generation of multiple vector beams on a single SLM," Opt. Express **25**, 25697 (2017).
83. P. Li, Y. Zhang, S. Liu, C. Ma, L. Han, H. Cheng, and J. Zhao, "Generation of perfect vectorial vortex beams," Opt. Lett. **41**, 2205 (2016).
84. I. Moreno, M. M. Sanchez-Lopez, K. Badham, J. A. Davis, and D. M. Cottrell, "Generation of integer and fractional vector beams with *q*-plates encoded onto a spatial light modulator," Opt. Lett. **41**, 1305 (2016).
85. A. Lohrmann, C. Perumgatt, and A. Ling, "Manipulation and measurement of quantum states with liquid crystal devices," Opt. Express **27**, 13765 (2019).
86. E. Nagali, F. Sciarrino, F. De Martini, L. Marrucci, B. Piccirillo, E. Karimi, and E. Santamato, "Quantum information transfer from spin to orbital angular momentum of photons," Phys. Rev. Lett. **103**, 013601 (2009).
87. A. Forbes, A. Aiello, and B. Ndagano, "Classically entangled light," Prog. Opt. **64**, 99 (2019).
88. N. Korolkova and G. Leuchs, "Quantum correlations in separable multi-mode states and in classically entangled light," Reports Prog. Phys. **82**, 056001 (2019).
89. J. H. Eberly, X. Qian, A. Al Qasimi, H. Ali, M. A. Alonso, R. Gutiérrez-Cuevas, B. J. Little, J. C. Howell, T. Malhotra, and A. N. Vamivakas, "Quantum and classical optics–emerging links," Phys. Scr. **91**, 063003 (2016).
90. E. Karimi and R. W. Boyd, "Classical entanglement?" Science **350**, 1172 (2015).
91. T. Stav, A. Faerman, E. Maguid, D. Oren, V. Kleiner, E. Hasman, and M. Segev, "Quantum entanglement of the spin and orbital angular momentum of photons using metamaterials," Science **361**, 1101 (2018).
92. Y. Shen, I. Nape, X. Yang, X. Fu, M. Gong, D. Naidoo, and A. Forbes, "Creation and control of high-dimensional multi-partite classically entangled light," Light Sci. Appl. **10**, 50 (2021).
93. B. Ndagano, B. Perez-Garcia, F. S. Roux, M. McLaren, C. Rosales-Guzman, Y. Zhang, O. Mouane, R. I. Hernandez-Aranda, T. Konrad, and A. Forbes, "Characterizing quantum channels with non-separable states of classical light," Nat. Phys. **13**, 397 (2017).
94. V. Parigi, V. D'Ambrosio, C. Arnold, L. Marrucci, F. Sciarrino, and J. Laurat, "Storage and retrieval of vector beams of light in a multiple-degree-of-freedom quantum memory," Nat. Commun. **6**, 7706 (2015).
95. X. Li, X. Liu, Z.-Q. Zhou, C.-F. Li, and G.-C. Guo, "Solid-state quantum memory for hybrid entanglement involving three degrees of freedom," Phys. Rev. A **101**, 052330 (2020).
96. V. D'Ambrosio, G. Carvacho, F. Graffitti, C. Vitelli, B. Piccirillo, L. Marrucci, and F. Sciarrino, "Entangled vector vortex beams," Phys. Rev. A **94**, 030304 (2016).
97. A. Sit, F. Bouchard, R. Fickler, J. Gagnon-Bischoff, H. Larocque, K. Heshami, D. Elser, C. Peuntinger, K. Günthner, B. Heim, C. Marquardt, G. Leuchs, R. W. Boyd, and E. Karimi, "High-dimensional intracity quantum cryptography with structured photons," Optica **4**, 1006 (2017).
98. F. Graffitti, V. D'Ambrosio, M. Proietti, J. Ho, B. Piccirillo, C. de Lisio, L. Marrucci, and A. Fedrizzi, "Hyperentanglement in structured quantum light," Phys. Rev. Res. **2**, 043350 (2020).
99. C. Rosales-Guzmán, N. Bhebhe, N. Mahonisi, and A. Forbes, "Multiplexing 200 spatial modes with a single hologram," J. Opt. **19**, 113501 (2017).
100. E. Otte, K. Tekce, and C. Denz, "Spatial multiplexing for tailored fully-structured light," J. Opt. **20**, 105606 (2018).
101. A. Trichili, C. Rosales-Guzmán, A. Dudley, B. Ndagano, A. Ben Salem, M. Zghal, and A. Forbes, "Optical communication beyond orbital angular momentum," Sci. Rep. **6**, 27674 (2016).
102. E. Otte, C. Rosales-Guzmán, B. Ndagano, C. Denz, and A. Forbes, "Entanglement beating in free space through spin-orbit coupling," Light Sci. Appl. **7**, 18009 (2018).
103. F. Cardano, M. Maffei, F. Massa, B. Piccirillo, C. de Lisio, G. De Filippis, V. Cataudella, E. Santamato, and L. Marrucci, "Statistical moments of quantum-walk dynamics reveal topological quantum transitions," Nat. Commun. **7**, 11439 (2016).
104. A. D'Errico, F. Cardano, M. Maffei, A. Dauphin, R. Barboza, C. Esposito, B. Piccirillo, M. Lewenstein, P. Massignan, and L. Marrucci, "Two-dimensional topological quantum walks in the momentum space of structured light," Optica **7**, 108 (2020).
105. D. Cozzolino, B. Da Lio, D. Bacco, and L. K. Oxenløwe, "High-dimensional quantum communication: benefits, progress, and future challenges," Adv. Quantum Technol. **2**, 1900038 (2019).
106. A. Gratsea, F. Metz, and T. Busch, "Universal and optimal coin sequences for high entanglement generation in 1D discrete time quantum walks," J. Phys. A **53**, 445306 (2020).
107. T. Giordani, E. Polino, S. Emiliani, A. Suprano, L. Innocenti, H. Majury, L. Marrucci, M. Paternostro, A. Ferraro, N. Spagnolo, and F. Sciarrino,

"Experimental engineering of arbitrary qudit states with discrete-time quantum walks," Phys. Rev. Lett. **122**, 020503 (2019).
108. T. Giordani, L. Innocenti, A. Suprano, E. Polino, M. Paternostro, N. Spagnolo, F. Sciarrino, and A. Ferraro, "Entanglement transfer, accumulation and retrieval via quantum-walk-based qubit–qudit dynamics," New J. Phys. **23**, 023012 (2021).
109. T. Giordani, A. Suprano, E. Polino, F. Acanfora, L. Innocenti, A. Ferraro, M. Paternostro, N. Spagnolo, and F. Sciarrino, "Machine learning-based classification of vector vortex beams," Phys. Rev. Lett. **124**, 160401 (2020).
110. F. Bouchard, A. Sit, Y. Zhang, R. Fickler, F. M. Miatto, Y. Yao, F. Sciarrino, and E. Karimi, "Two-photon interference: the Hong–Ou–Mandel effect," Rep. Prog. Phys. **84**, 012402 (2021).
111. E. Nagali, L. Sansoni, F. Sciarrino, F. De Martini, L. Marrucci, B. Piccirillo, E. Karimi, and E. Santamato, "Optimal quantum cloning of orbital angular momentum photon qubits through Hong–Ou–Mandel coalescence," Nat. Photon. **3**, 720 (2009).
112. V. D'Ambrosio, G. Carvacho, I. Agresti, L. Marrucci, and F. Sciarrino, "Tunable two-photon quantum interference of structured light," Phys. Rev. Lett. **122**, 013601 (2019).
113. M. Hiekkamäki and R. Fickler, "High-dimensional two-photon interference effects in spatial modes," Phys. Rev. Lett. **126**, 123601 (2021).
114. S. G. Lukishova, A. C. Liapis, L. J. Bissell, G. M. Gehring, and R. W. Boyd, "Single-photon experiments with liquid crystals for quantum science and quantum engineering applications," Liq. Cryst. Rev. **2**, 111 (2014).
115. S. G. Lukishova, A. C. Liapis, H. Zhu, E. Hebert, K. Kuyk, S. Choudhary, R. W. Boyd, Z. Wang, and L. J. Bissell, "Plasmonic nanoantennas with liquid crystals for nanocrystal fluorescence enhancement and polarization selectivity of classical and quantum light sources," Mol. Cryst. Liq. Cryst. **657**, 173 (2017).
116. W. Fu, Y. Zhou, Y. Yuan, T. Lin, Y. Zhou, T. Zeng, H. Huang, F. Fan, and S. Wen, "Symmetric Airy vortex and symmetric Airy vector beams," Liq. Cryst. **48**, 484 (2021).
117. T. Bauer, P. Banzer, E. Karimi, S. Orlov, A. Rubano, L. Marrucci, E. Santamato, R. W. Boyd, and G. Leuchs, "Observation of optical polarization Möbius strips," Science **347**, 964 (2015).
118. Y. Intaravanne and X. Chen, "Recent advances in optical metasurfaces for polarization detection and engineered polarization profiles," Nanophotonics **9**, 1003 (2020).
119. Y. Hu, X. Ou, T. Zeng, J. Lai, J. Zhang, X. Li, X. Luo, L. Li, F. Fan, and H. Duan, "Electrically tunable multifunctional polarization-dependent metasurfaces integrated with liquid crystals in the visible region," Nano Lett. **21**, 4554 (2021).
120. T. Wei, P. Chen, M. Tang, G. Wu, Z. Chen, Z. Shen, S. Ge, F. Xu, W. Hu, and Y. Lu, "Liquid-crystal-mediated active waveguides toward programmable integrated optics," Adv. Opt. Mater. **8**, 1902033 (2020).
121. Y. Liu, W. Chen, J. Tang, X. Xu, P. Chen, C.-Q. Ma, W. Zhang, B.-Y. Wei, Y. Ming, G.-X. Cui, Y. Zhang, W. Hu, and Y.-Q. Lu, "Switchable second-harmonic generation of Airy beam and Airy vortex beam," Adv. Opt. Mater. **9**, 2001776 (2021).